The 9th European Congress on Computational Methods in Applied Sciences and Engineering
ECCOMAS Congress 2024
3 – 7 June 2024, Lisboa, Portugal

REVIEW AND CHALLENGES FOR A REALISTIC NUMERICAL SHM BENCHMARK

F. MARAFINI[1], G. ZINI[1], A. BARONTINI[2], M. BETTI[1], G. BARTOLI[1], N. MENDES[2], A. CICIRELLO[3]

[1] Department of Civil and Environmental Engineering (DICEA), University of Florence, Florence, Italy

[2] ISISE, Department of Civil Engineering, University of Minho, Guimarães, Portugal

[3] Department of Engineering, University of Cambridge, Cambridge, UK

Key words: Numerical benchmark, Data generation, Damage detection, Sensor Fault, Environmental and Operational Variability

Summary: This paper presents a comprehensive review and critical discussion of existing numerical benchmarks in Structural Health Monitoring (SHM), focusing on the challenges and limitations of accurately simulating real-world conditions. The review presents the evolution of benchmarks from simplistic models to more complex simulations that aim to replicate operational and environmental variabilities (EOVs) and various damage scenarios. Despite these advancements, benchmarks currently available in the literature have yet to incorporate additional phenomena, such as long-term environmental effects and sensor faults or malfunctions. A proposal for a new benchmark integrating these factors into the simulation process is presented in the paper. This benchmark aims to facilitate comprehensive testing and validation of SHM techniques in a controlled, realistic numerical setup by including both fast and slow-varying damage scenarios and sensor malfunctions. The proposed framework is applied to a simple structural model—a steel beam subject to varying loads and environmental conditions—demonstrating its potential to simulate a wide range of real-world phenomena.

1. INTRODUCTION

In the field of Structural Health Monitoring (SHM) of civil structures and infrastructures, the acquisition of large amounts of data has become a regular practice. Measured or derived quantities from monitored data are chosen with the objective of operating damage identification (DI) for effects in the short-term (fast-varying) and in the long-term due to the natural ageing of the structure over time (slow-varying). However, the data collected is affected by the variability of environmental and operations conditions (EOVs). Air temperature and humidity variations act on structural components, and the changes in use or maintenance activities in the structure cause variations of the structure behaviour under “nominally identical” operational loading conditions. Noise and the fault or malfunction of the measurement system can also affect the monitored data. These effects are sources of uncertainty and variability and could overlap and mask one another, hindering the interpretability of the results and the identification

of the presence of damage.
In order to test the applicability of damage identification techniques and evaluate the content of monitored data, experimental benchmark studies for SHM and, more broadly, for structural dynamics applications have been developed and published with their data made publicly available from the first and most famous Z24 bridge [1], [2], to the most recent applications on aircraft structures [3]. Experimental datasets are limited by time and economic constraints. Therefore, numerical benchmarks were also developed, either starting from simple analytical formulations of mechanical systems [4] or expanding on existing experimental studies [5]. The focus of SHM numerical benchmark research has been the simulations of large quantities of reference undamaged data, with the additional simulation of damage scenarios due to stiffness reduction and the account of variations in the loading conditions. In such studies, environmental variabilities or long-term damage effects were rarely considered and never in combination with sensor fault or malfunction data in the simulations.
The present work reviews existing numerical benchmarks for SHM application, followed by a description of the challenges in generating realistic synthetic SHM data and the strategies to address them. This discussion is supported by a case study involving the 4-year simulated monitoring of a simple structural system: a steel beam, modelled as a simple Single Degree of Freedom system (SDOF) for the dynamic analysis and a fixed-fixed Euler-Bernoulli beam for the static analysis. This study accounts for EOVs, sensor faults or malfunctions, and fast-varying or slow-varying damage scenarios.

2. SHM NUMERICAL BENCHMARK

Previous research efforts have developed benchmark experimental and numerical datasets to study SHM problems. The contributions in terms of numerical benchmarks are summarised in Table 1. Initially, numerical applications were developed to either generate specific quantities [4] or to build a calibrated model to reproduce the experimental setups [6], [7], [8], [9]. Later, the limited availability of real-world damage data and the economic constraints of damaging prototypes and simulating EOVs led to the generation of synthetic data [10], [11], providing an improved control of uncertainties and interferences if compared to experimental applications.
In terms of environmental variabilities, the lack of general theoretical models describing the effects of temperature and humidity on material properties has led few studies to include them. In particular, Tatsis and Chatzi's data generation benchmark allows for the introduction of the variability of the steel Young's Modulus given a specific temperature but relies on the presence of experimental data describing the relationship [11]. When benchmarking is done to study prefabricated and industrially produced structural elements, the accounts for humidity and temperature variability in terms of impact on the material properties are more accessible, for example, on the numerical and experimental benchmark of a wind turbine blade from Tatsis et al. [12]. Finally, temperature effects and weather conditions are commonly measured when a full-scale experimental structure is set up, but the monitored environmental data are not yet used as input for the numerical application. Percentage reduction or increase of material properties such as Young's modulus or density is often used to obtain the corresponding variability in the modal properties referencing real case studies [5].
In terms of operational conditions, ambient vibration simulated as a white Gaussian noise is most commonly used as a dynamic input, and the variability of the applied static load [10], the

impact of shakers or the presence of moving loads are also accounted for in numerical simulations [11]. Long-term damage effects are introduced only by Tatsis et al. in a numerical benchmark, reducing the structural section to simulate corrosion wastage [11] and adding mass to model icing accretion [12]. The simulation of sensor faults and malfunction is not included in combination with damage scenarios and EOVs in any numerical benchmarks in the literature. There are still significant challenges in developing numerical benchmarks regarding the over-simplification in simulations, with the risk of not capturing the full complexity of real-world conditions and material behaviours and the limited accuracy of numerical models, which rely on the quality of input parameters, but further steps can be made to include as many sources of variability and uncertainty as possible in the data simulations.

Table 1: Review of numerical benchmark studies

#	Reference	Year	Structure	Objective	OVs	FVD
1	Worden et al. [4]	1996	Multi Degree of Freedom (MDOF) Mechanical System	Novelty detection using the transmissibility function as a feature	Harmonic excitation	1, 10 and 50% stiffness reduction
2*	Spencer et al. [6] - [7]	1999	SAC Phase II Steel Moment Frame	Test control strategies after strong motion earthquakes	Ground acceleration	Stiffness reduction corresponding to an 18% reduction in frequency
3	Johnson et al. [8]	2002	IASC-ASCE SHM 2x2bay steel frame	Evaluation of SHM methods	White Gaussian Noise (WGN) Shakers	6 scenarios with braces removal or bolts loosening
4*	Burkett Thesis [9]	2003	IABMAS 1-2 span bridge	Test damage detection algorithms	WGN Hammer impact Shakers	Reduced stiffness Boundary condition change
5	Tiso et al. [10]	2017	Two offset cantilevered beams	Complex nonlinear dynamics for system identification	Load amplitude variations	No damage scenarios
6	Tatsis, Chatzi [11]	2019	2-span steel beam	Validation of decision-making tools	WGN Deterministic moving load	6 scenarios with stiffness reduction
7	Tatsis et al. [12]	2021	Wind turbine blade	Condition assessment of a wind turbine blade	Rotor speed changes	Cracks openings simulated as local stiffness reduction
8	Vlachas et al. [13]	2021	Two-story steel frame structure with Bouc-Wen hysteretic links	Validations of SHM, model reduction, and structural identification methods	Ground motion excitation scenarios	Bouc-Wen model parameter variations for strength and stiffness deterioration
9*	Svendsen et al. [5]	2022	Steel truss bridge (Hell Bridge Test Arena)	Hybrid SHM for DI on steel bridges	WGN	Stiffness reduction in connections

* The study is also experimental

_ If the authors' names are underlined, the data is available for public use

3. The numerical benchmark

The proposed numerical benchmark is designed to address some of the open challenges in generating synthetic data and developing viable numerical strategies for Structural Health Monitoring (SHM). A simple but informative case study is utilised: a fixed steel beam modelled as a Single Degree of Freedom (SDOF) system for the simulated dynamic monitoring and an Euler Bernoulli beam for the simulated static monitoring. The selection of an SDOF system is based on its capacity to balance computational simplicity with the ability to capture key behaviours in illustrative measured SHM data. It serves as an appropriate framework for examining all the components interacting in the data, as discussed in the previous section.
Simulated monitoring is generated over four years, considering single static hourly acquisitions of the beam midspan deflection and three-minute-long length acceleration time histories. This setup includes the effects on the measured data of the following key phenomena or occurrences:

- the variation in time of the input operational static load;
- the variation in time of the ambient vibration frequency content and amplitude;
- the partial effect of the environmental conditions' variability on the linear properties of the structure materials, applied with the use of an empirical relationship between the linear stiffness of steel and temperature;
- the effect of sudden/fast damage on the data (shift), modelled as a sudden stiffness decay, and of progressive/slow damage (trend), simulating accelerated corrosion conditions decreasing the area of the beam and, therefore, its stiffness and mass;
- the effect of typical sensor malfunctions is applied a posteriori to the simulated data.

Therefore, the structural response variable, denoted as $x(t)$ (see Eq. (1)), includes for both dynamic and static simulations the cumulative effect of the variation of temperature $T(t)$ as an exogenous environmental factor of the variation of the operational load $\mathrm{l}(t)$, and two types of damage effects: $d_{\mathrm{fast}}(t)$ for sudden events (e.g., stiffness decay indicative of rapid damage occurrence), and $d_{\mathrm{slow}}(t)$ for progressive damage (e.g., corrosion). Sensor malfunction or failure is represented by $g(t)$, capturing the anomalies in data not directly related to the structural health itself, applied at this time only to the acceleration data. The term $\varepsilon(t)$ is included to account for potential random errors or noise within the measurements, modelled as Gaussian white noise.

$$\begin{aligned} x_{dyn}(t) &= f\left(T(t), l(t), d_{fast}, d_{slow}(t), g(t)\right) + \varepsilon(t) \\ x_{stat}(t) &= f\left(T(t), l(t), d_{fast}, d_{slow}(t)\right) + \varepsilon(t) \end{aligned} \tag{1}$$

In the remainder of this paper, the reference structure is described in terms of geometry, materials, and constraints, together with the above-mentioned simulated effects of operational and environmental variability, damage, and sensor fault.

3.1. Geometry, materials, constraints

The benchmark model is designed to balance the simulation of conditions as realistically as possible with computational cost and complexity, thereby providing a comprehensive but manageable dataset simulating structural behaviour. The benchmark model for this study consists of a steel IPE400 beam paired with a concrete slab, representing a typical residential structure component. The beam measures 6 meters in length in S235 grade steel. The beam's Young's modulus is 210,000 MPa, with a density of 7,850 kg/m³. The beam is designed to support the slab's self-weight and additional non-structural permanent loads, creating a total

dead load of 28.72 kN/m and a reference value for the live load of 15.00 kN/m. The beam is fixed at both ends, allowing no horizontal or vertical displacement or rotation at the supports. The chosen benchmark setup, while simplified, effectively captures the structural response under EOVs and ensures that the model remains sufficiently realistic while being computationally efficient and accessible for testing SHM methods.

3.2. Environmental and operational variability

Simulating EOVs numerically presents significant challenges, particularly in achieving a balance between the realism of simulated responses and the practical constraints of numerical simulations. Research on the simulation and mathematical formulation of such effects is either limited to extreme events (e.g. material behaviour under high temperatures [14], [15]) not considering the operational range or extremely specific serviceability issues (e.g. the simulation of human-induced vibrations [16]). Nonetheless, the distinction between the effect of EOVs and the presence of damage is key in SHM applications for DI.

In this case study, these challenges are addressed by combining artificial, numerically generated responses with real monitored environmental data to produce realistic results. Similarly, operational variability is recreated as realistically as possible by referencing ranges of operational values obtained from established codes and literature, balancing complexity and adherence to reality.

In order to simulate the effect of environmental conditions, the Young's Modulus E of steel is made vary for each simulation as per Eq. (2), in which E_0 is the value of E at 20°C, T^* the surface temperature, α an amplification parameter is added to scale the temperature effect. The constants e_1, e_2, e_3, and e_4 are obtained experimentally in [17].

$$E(T) = E_0\,(1 - \alpha \cdot T^*)\exp\left(-\frac{1}{2}\left(\frac{T^*}{e_3}\right)^{e_1} - \frac{1}{2}\left(\frac{T^*}{e_4}\right)^{e_2}\right) \tag{2}$$

Temperature data were obtained for four consecutive years from 2020 from a sensor in the vicinity of the University of Florence. The data obtained shows the clear presence of seasonality and its effects on the structural stiffness of steel. It is to be noted that the relationship describes a nonlinear effect, but in the range of operative temperatures, it is sufficiently close to a simple linear dependency of stiffness from temperature. Furthermore, an amplification parameter is included to increase the effect of the environmental variability (EV) on the Young's Modulus to accentuate the effect of temperature ($\alpha = 0.0015$ in Eq. (2)) (see Figure 1).

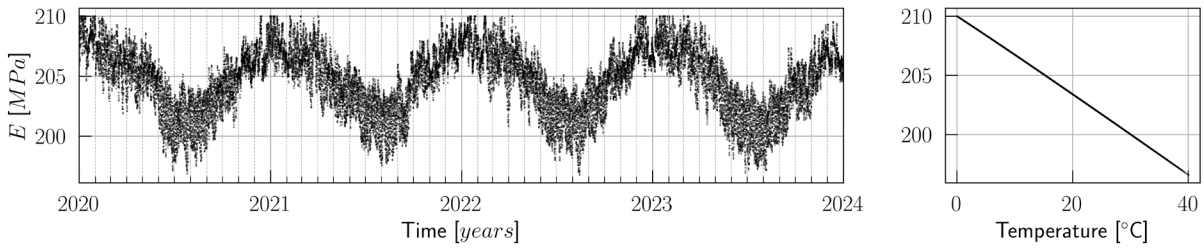

Figure 1: Simulated variability of the steel Young's Modulus with temperature in time (left) and the relationship between E and T (right).

In order to include the operational variability, the permanent load l_{Perm} due to self-weight is calculated deterministically as a constant, but the live load l_{Live} is not considered as time-invariant. It is, in fact, a sum of two components: one sustained (or long-term l_{Llt}) and one

intermitted (or short-term l_{Lst}), evaluated with a probabilistic approach according to the Probability Model Code of the Joint Committee on Structural Safety (JCSS) [18]. This approach considers time variability due to occupancy changes and possible crowded events. The total load acting on the structure is a combination of these components, considering for the simulation a serviceability limit state combination [19], as per Eq. (3).

$$l(t) = 1.0 \cdot l_{Perm} + 1.0 \cdot (l_{Live} = \left(l_{Llt}(t) + l_{Lst}(t) \right)) \quad (3)$$

The sustained live-load is modelled as a stationary process, while the intermitted live-load with occasional high-intensity events as a non-stationary process, specifically using a Poisson spike process. The intensity and occurrence are determined by sampling from statistical distributions defined with specific parameters from [19]. Figure 2 shows the profile of the total live load.

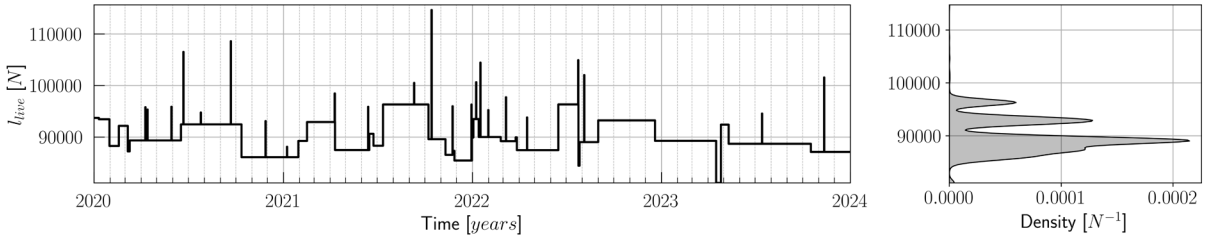

Figure 2: Simulated variability of the applied live load in time (left) and variation of the live load vs density (right).

3.3. Static and dynamic response simulation

The static monitoring simulation is operated by calculating the single value of the deflection at mid-span for the reference fixed-fixed Euler-Bernoulli beam under the time-varying uniformly distributed load. The deflection results for the undamaged condition simulated for the 4 years of monitoring as shown in Figure 3.

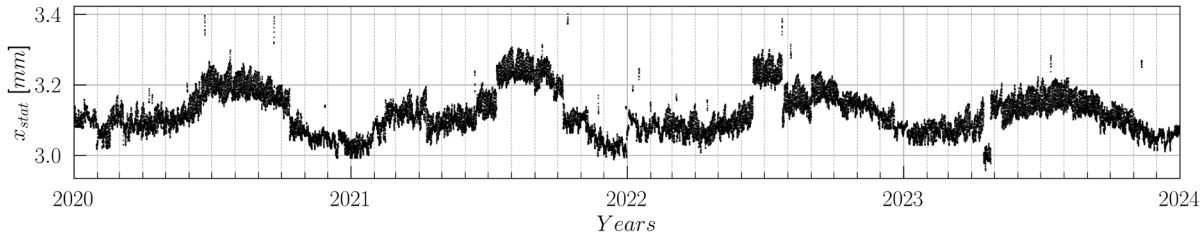

Figure 3: Simulated static monitoring: mid-span deflection with the effect of EOVs

The dynamic monitoring simulation is operated under ambient vibration conditions, differentiating the sources of dynamic input by superimposing different WGN signals. A band-pass filter is applied to two different signals to selectively target specific frequency bands corresponding to the effects of human activities (1.2 ÷ 4.8 Hz) and vehicular traffic (7 ÷ 15 Hz). The signals are generated with a different amplitude randomly sampled (between 5e-3 – 5e-1 mm/s^2, and 1e-6 ÷ 2e-4 mm/s^2, respectively) and then summed to obtain a different input, ω_{AV} for each simulated acquisition.

Given the equivalent stiffness k, mass m, damping coefficient c, the defined input vibration ω_{AV}, and the addition of measurement noise ω_M, the dynamic response is calculated with a state-space approach, starting from the equation of motion describing the dynamic behaviour

of the SDOF. To convert this second-order differential equation into a form suitable for state-space analysis, the state variables, $x_1 = x(t)$, $x_2 = \dot{x}(t)$ corresponding respectively to displacement and acceleration, were substituted in the equation of motion leading to solve a system of two first-order differential equations (see Eq. (4)).

$$\dot{x}(t) = \begin{bmatrix} 0 & 1 \\ -\frac{k}{m} & -\frac{c}{m} \end{bmatrix} \begin{bmatrix} x_1 \\ x_2 \end{bmatrix} + \begin{bmatrix} 0 \\ \frac{1}{m} \end{bmatrix} (\omega_{AV}\, m) + \begin{bmatrix} 0 \\ \frac{1}{m} \end{bmatrix} \omega_M \tag{4}$$

From each simulated acceleration, it is then possible to extract derived quantities commonly used in SHM applications, for example, the natural frequency of the structure (see Figure 4).

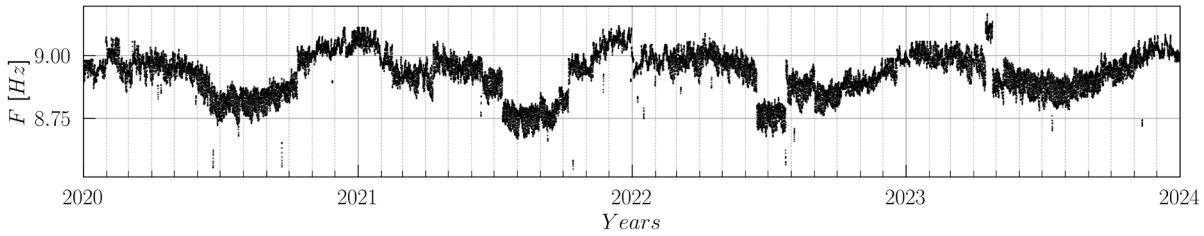

Figure 4: Time history of extracted natural frequency with the effect of EOVs and additional noise.

3.4. Fast and slow varying damage

Simulating damage numerically needs to account for the diverse nature of damage scenarios and the complexity of accurately capturing their effects. Fast-varying damage (FVD) is particularly difficult to model because it encompasses a wide range of potential defects or events, each with unique characteristics. Additionally, it is not guaranteed that real damage will directly impact the quantities measured by SHM systems, adding another layer of uncertainty to simulations. On the other hand, slow-varying damage (SVD) occurs gradually over an extended period, making it challenging to detect and model. However, accurately simulating SVD is crucial, as ageing effects might be overlooked if they are learned as part of the training in DI approaches. Moreover, to produce a manageable dataset for analysis, these slow processes need to be artificially accelerated.

In the proposed numerical benchmark, FVD is modelled as a localised sudden shift in stiffness, as commonly done in numerical SHM benchmarks. SVD is instead modelled as diffused, simulating the effects of corrosion. This is applied as a loss of mass to the beam due to thickness reduction of the whole area at a specific rate and a loss of stiffness due to the reduction of the section inertia at the same identified rate. The rate of loss references a specific relationship representing the interaction with environmental variables. The model proposed in 2007 [20] is used to define the corrosion rate given the environment of the beam, according to the relationship in Eq. (5). Here, d represents the corrosion loss $[\mu m]$ as a function of t, the exposure time $[years]$. TOW is the annual time of wetness $\left[\frac{h}{year}\right]$, namely the fraction of time that the metal surface remains wet. For simplicity, the TOW is approximated as the time in which the RH is greater than 80% and the temperature is greater than 0°C [21]. T is the temperature [°C] and A, B, D, E, F, G, H, J and T_0 are coefficients proposed in [20] and adapted for the present case.

$$d(t) = A \cdot t^B \cdot \left(\frac{TOW}{C}\right)^D \cdot \left(1 + \frac{[SO_2]}{E}\right)^F \cdot \left(1 + \frac{[Cl]}{G}\right)^H \cdot e^{J(T + T_0)} \tag{5}$$

3.5. Sensor faults and malfunction simulation

The accurate simulation of sensor faults and malfunctions has yet to be introduced in the development of numerical benchmarks for SHM. These faults can significantly impact the integrity of the data collected, potentially leading to incorrect assessments of structural health if not properly identified and managed. The simulation of sensor faults or malfunctions is operated a posteriori on the acceleration signals in the proposed benchmark. The possible faults/malfunctions are classified as per Table 2, according to literature research [22], [23], [24] and real data observations.

Seven classes of sensor faults/malfunctions are identified:

- drifting (D) due to temperature changes or mechanical wear relaxation, characterized by a change in the sensor's output over time;
- the presence of spikes (S) due to power surges and weather disturbances, introduced into the signal by adding a large amplitude value at a specific time instant;
- bias or shift (B) due to power interruptions and incorrect recalibrations of the instruments, introducing a constant offset to the sensor output;
- gain (G), due to the incorrect design of the sensor or change in sensitivity requirements of the sensor, shown as amplification or attenuation of the signal;
- noise (N), due to electronic noise and environmental factors, simulated with a superimposed Gaussian noise;
- the interruption of sensor recording resulting in missing data (M), resulting in gaps in the time series;
- cable detachment (C), due to mechanical failure or human interaction, characterised by a sinusoidal wave with a rapidly decreasing amplitude, simulating the sensor becoming disconnected.

For each classified type, a short description is provided in terms of the effect in the time domain and a mathematical formulation for the simulation. In each formulation $a(t)$ represents the original signal and $a_*(t)$, with the appropriate subscript, represents its updated version after the application of the fault or malfunction, dependent on the time vector t. The term s_* is a scale factor representing the magnitude of each malfunction (i.e. the shift, the maximum value of the spike, the scale factor for the gain, etc.), each s_* factor is calibrated according to the magnitude of the measured accelerations. l_s is the length of the signal, t_{st} represents the point in the time history at which the fault or malfunction is applied, generally randomly sampled starting from 10 seconds or recording onwards, t_{end} the end of the signal time history. Specific durations are defined for spikes and cable detachment as Δt_*. $\eta(t)$ represents a Gaussian noise with zero mean of zero and a standard deviation s_N reflecting the noise level in the sensor. Finally, in the cable detachment simulation, s_C is the initial amplitude of the sinusoidal wave, f_C its frequency, and λ_C its decay rate, which causes the amplitude to decrease rapidly after the detachment begins. An example of the simulated sensor faults and malfunctions is provided in Figure 5.

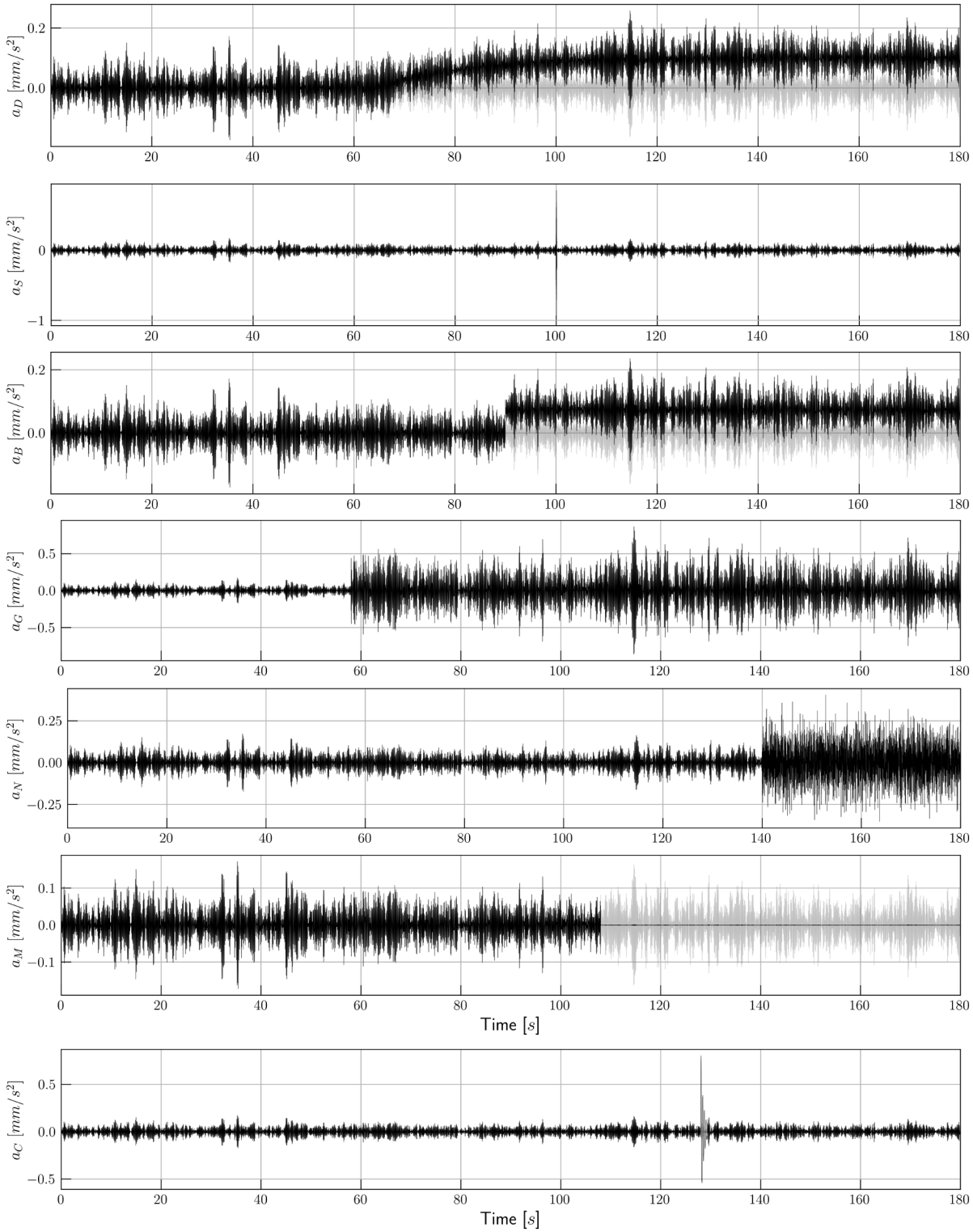

Figure 5: Example of generated sensor fault, in order from top to bottom: (1) drift, (2) spikes, (3) bias, (4) gain, (5) noise, (6) missing data, and (7) cable detachment.

Table 2: Typologies of sensor faults simulated

Class	Description	Formulation
Drifting	Decay of the signal, up to a shifted mean	$a_D(t) = a(t) + s_D \cdot \exp\left(-\frac{t}{\frac{l_s}{10}}\right) + s_D, \quad t \in [t_{st}, t_{end}]$
Spike	Sharp changes over or under 3std	$a_S(t) = a(t) + s_S \cdot (\Delta t_{spike}), \quad t \in [\Delta t_{spike}]$
Bias	Fixed offset	$a_B(t) = a(t) + s_B, \quad t \in [t_{st}, t_{end}]$
Gain	Output scaled by a factor	$a_G(t) = a(t) \cdot s_G, \quad t \in [t_{st}, t_{end}]$
Noise	Gaussian superposition	$a_N(t) = a(t) + \eta(t), \quad t \in [t_{st}, t_{end}]$
Missing data	Discontinuities and gaps in the signal	$a_M(t) = null\ or\ missing, \quad t \in [t_{st}, t_{end}]$
Cable detachment	Sinusoidal wave with fast decreasing amplitude	$a_C(t) = s_C \sin(2\pi f_C t) \exp(-\lambda_C t), \quad t \in [\Delta t_{detach}]$

3.6. Data generation

From the numerical benchmark setup described before, it was possible to generate a series of datasets containing different levels and types of damage, accounting for EOVs effect, measurement noise and sensor faults or malfunctions. The numerical nature of the benchmark allowed to exploit the computing power of parallel computing, generating a large amount of data for years of monitoring in a few hours (e.g. four years of simulated acceleration measurements can be generated in three hours using the full power of an Intel Core i7-8750H processor, 12 cores, 2.2 GHz, implementing the simulation in Python 3.11 using the Ray package). Two examples of frequency time histories extracted from the generated data are shown in Figure 6 with fast-varying damage (decrease of 10% in k), and slow-varying damage (corrosion rate equal to 47.03 [μm/year] multiplied by 10).

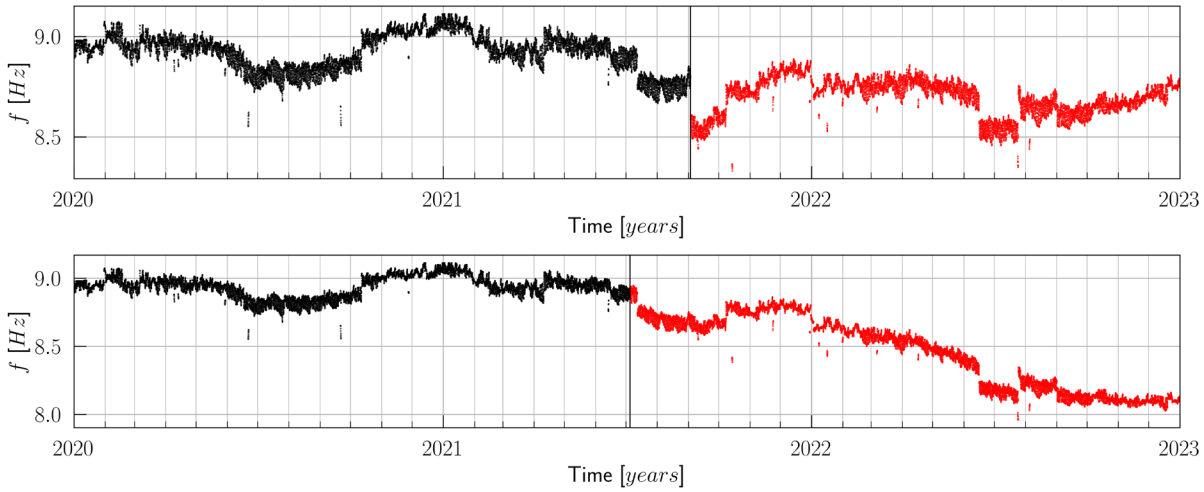

Figure 6: Plot of the effect of FVD and SVD on the extracted frequency.

4. CONCLUSIONS

This paper reviewed existing numerical benchmarks for SHM and proposed a new, comprehensive one designed to highlight the inherent challenges in developing artificial SHM data. The objective of this work is to underscore the complexities involved in accurately simulating the various factors that impact SHM data, including EOVs, FVD and SVD and sensor faults and malfunctions. Each of these factors presents specific difficulties in the numerical simulation, such as the gradual nature of structural degradation or the possible overlap between damage and sensor faults effects. To address these challenges, the proposed benchmark offers solutions to provide an approach that is as realistic as possible for SHM data generation. The incorporation of ageing damage and sensor faults and malfunctions extends what was found in existing methods in the literature, broadening the spectrum of effects that can be modelled in a synthetic SHM dataset.
In conclusion, the proposed benchmark design allowed to address the complexities of SHM data generation, underscoring currently unexplored limitations. The critical considerations operated on synthetic data generation will facilitate a more comprehensive testing and validation of SHM methodologies and damage-sensitive feature extraction and selection, enhancing their applicability and reliability in real-world scenarios.

REFERENCES

[1] A. Teughels and G. D. Roeck, ‘Damage Assessment of the Z24 bridge by FE Model Updating’.
[2] J. Maeck and G. De Roeck, ‘Description of Z24 bridge’, *Mechanical Systems and Signal Processing*, vol. 17, no. 1, pp. 127–131, Jan. 2003, doi: 10.1006/mssp.2002.1548.
[3] M. Haywood-Alexander *et al.*, ‘Full-scale modal testing of a Hawk T1A aircraft for benchmarking vibration-based methods’, *Journal of Sound and Vibration*, vol. 576, p. 118295, Apr. 2024, doi: 10.1016/j.jsv.2024.118295.
[4] K. Worden, ‘Structural Fault Detection Using a Novelty Measure’.
[5] B. T. Svendsen, G. T. Frøseth, O. Øiseth, and A. Rønnquist, ‘A data-based structural health monitoring approach for damage detection in steel bridges using experimental data’, *J Civil Struct Health Monit*, vol. 12, no. 1, pp. 101–115, Feb. 2022, doi: 10.1007/s13349-021-00530-8.
[6] B. F. Spencer, R. E. Christenson, and S. J. Dyke, ‘Next Generation Benchmark Control Problem for Seismically Excited Buildings’, 1999.
[7] Y. Ohtori, R. E. Christenson, B. F. Spencer, and S. J. Dyke, ‘Benchmark Control Problems for Seismically Excited Nonlinear Buildings’, *J. Eng. Mech.*, vol. 130, no. 4, pp. 366–385, Apr. 2004, doi: 10.1061/(ASCE)0733-9399(2004)130:4(366).
[8] E. A. Johnson, H. F. Lam, L. S. Katafygiotis, and J. L. Beck, ‘Phase I IASC-ASCE Structural Health Monitoring Benchmark Problem Using Simulated Data’, *J. Eng. Mech.*, vol. 130, no. 1, pp. 3–15, Jan. 2004, doi: 10.1061/(ASCE)0733-9399(2004)130:1(3).
[9] J. L. Burkett, ‘Benchmark Studies For Structural Health Monitoring Using Analytical And Experimental Models’.
[10] P. Tiso and J.-P. Noël, ‘A new, challenging benchmark for nonlinear system identification’, *Mechanical Systems and Signal Processing*, vol. 84, pp. 185–193, Feb. 2017, doi: 10.1016/j.ymssp.2016.08.008.

[11] K. Tatsis and E. Chatzi, 'A NUMERICAL BENCHMARK FOR SYSTEM IDENTIFI- CATION UNDER OPERATIONAL AND ENVIRONMENTAL VARIABILITY'.
[12] K. Tatsis, Y. Ou, V. K. Dertimanis, M. D. Spiridonakos, and E. N. Chatzi, 'Vibration-based monitoring of a small-scale wind turbine blade under varying climate and operational conditions. Part II: A numerical benchmark', *Struct Control Health Monit*, vol. 28, no. 6, Jun. 2021, doi: 10.1002/stc.2734.
[13] K. Vlachas, K. Tatsis, K. Agathos, A. R. Brink, and E. Chatzi, 'Two-story frame with Bouc-Wen hysteretic links as a multi-degree of freedom nonlinear response simulator'.
[14] W. Wang, B. Liu, and V. Kodur, 'Effect of Temperature on Strength and Elastic Modulus of High-Strength Steel', *J. Mater. Civ. Eng.*, vol. 25, no. 2, pp. 174–182, Feb. 2013, doi: 10.1061/(ASCE)MT.1943-5533.0000600.
[15] W. Kumar, U. K. Sharma, and M. Shome, 'Mechanical properties of conventional structural steel and fire-resistant steel at elevated temperatures', *Journal of Constructional Steel Research*, vol. 181, p. 106615, Jun. 2021, doi: 10.1016/j.jcsr.2021.106615.
[16] L. Cao, J. Li, Y. Frank Chen, and S. Huang, 'Measurement and application of walking models for evaluating floor vibration', *Structures*, vol. 50, pp. 561–575, Apr. 2023, doi: 10.1016/j.istruc.2023.02.073.
[17] M. Seif *et al.*, 'Temperature-Dependent Material Modeling for Structural Steels: Formulation and Application', National Institute of Standards and Technology, NIST TN 1907, Apr. 2016. doi: 10.6028/NIST.TN.1907.
[18] *JCSS Probabilistic Model Code Part 2: Load Models*, Guideline II, May 2021.
[19] A. Barocci, *Norme tecniche per le costruzioni 2018: le NTC 2018 (D.M. 17 gennaio 2018) e la loro applicazione: testo della norma, commento, confronto NTC 2008 e NTC 2018*. Santarcangelo di Romagna (RN): Maggioli, 2018.
[20] D. E. Klinesmith, R. H. McCuen, and P. Albrecht, 'Effect of Environmental Conditions on Corrosion Rates', *J. Mater. Civ. Eng.*, vol. 19, no. 2, pp. 121–129, Feb. 2007, doi: 10.1061/(ASCE)0899-1561(2007)19:2(121).
[21] L. Di Sarno, A. Majidian, and G. Karagiannakis, 'The Effect of Atmospheric Corrosion on Steel Structures: A State-of-the-Art and Case-Study', *Buildings*, vol. 11, no. 12, p. 571, Nov. 2021, doi: 10.3390/buildings11120571.
[22] A. Javaid *et al.*, 'Machine Learning Algorithms and Fault Detection for Improved Belief Function Based Decision Fusion in Wireless Sensor Networks', *Sensors*, vol. 19, no. 6, p. 1334, Mar. 2019, doi: 10.3390/s19061334.
[23] M. Ahmer, F. Sandin, P. Marklund, M. Gustafsson, and K. Berglund, 'Failure mode classification for condition-based maintenance in a bearing ring grinding machine', *Int J Adv Manuf Technol*, vol. 122, no. 3–4, pp. 1479–1495, Sep. 2022, doi: 10.1007/s00170-022-09930-6.
[24] A.-M. Oncescu and A. Cicirello, 'A Self-supervised Classification Algorithm for Sensor Fault Identification for Robust Structural Health Monitoring', in *European Workshop on Structural Health Monitoring*, vol. 253, P. Rizzo and A. Milazzo, Eds., in Lecture Notes in Civil Engineering, vol. 253. , Cham: Springer International Publishing, 2023, pp. 564–574. doi: 10.1007/978-3-031-07254-3_57.